REVIEWS

Journal of Semiconductors
(2019) 40, 111608
doi: 10.1088/1674-4926/40/11/111608

Recent progress on gas sensors based on graphene-like 2D/2D nanocomposites

Songyang Yuan[1] and Shaolin Zhang[1, 2, 3, †]

[1]Advanced Institute of Engineering Science for Intelligent Manufacturing, Guangzhou University, Guangzhou 510006, China
[2]School of Physics and Electronic Engineering, Guangzhou University, Guangzhou 510006, China
[3]Faculty of Electrical Engineering and Computer Science, Ningbo University, Ningbo 315211, China

Abstract: Two-dimensional (2D) nanomaterials have demonstrated great potential in the field of flexible gas sensing due to their inherent high specific surface areas, unique electronic properties and flexibility property. However, numerous challenges including sensitivity, selectivity, response time, recovery time, and stability have to be addressed before their practical application in gas detection field. Development of graphene-like 2D/2D nanocomposites as an efficient strategy to achieve high-performance 2D gas sensor has been reported recently. This review aims to discuss the latest advancements in the 2D/2D nanocomposites for gas sensors. We first elaborate the gas-sensing mechanisms and the collective benefits of 2D/2D hybridization as sensor materials. Then, we systematically present the current gas-sensing applications based on different categories of 2D/2D nanocomposites. Finally, we conclude the future prospect of 2D/2D nanocomposites in gas sensing applications.

Key words: gas sensor; 2D nanomaterials; 2D/2D nanocomposite; heterojunction; flexible sensor

Citation: S Y Yuan and S L Zhang, Recent progress on gas sensors based on graphene-like 2D/2D nanocomposites[J]. *J. Semicond.*, 2019, 40(11), 111608. http://doi.org/10.1088/1674-4926/40/11/111608

1. Introduction

Gas sensor is an electronic device that can qualitatively or quantificationally detect the specific gases, and has been widely used in many fields, such as indoor/outdoor gas monitoring, industrial control, agricultural production, medical diagnosis, and military and public safety[1–4]. Generally, conventional gas sensor materials are constructed by semiconducting metal oxides, conducting polymers, and carbon nanotubes[5, 6]. Among these, metal oxides are the most successfully commercialized sensing material owing to their ease of fabrication, high sensitivity and economical cost[7, 8]. However, their drawbacks including high-temperature operation, large power consumption, and low selectivity are also significant that render them inadequacy for the next-generation wearable sensor application. The conducting polymers-based sensors could be conducted at room temperature without extra power requirement but suffered from the degraded property in air, specifically in humidity[9]. The usage of carbon nanotubes could greatly lower the operating temperature of the sensor bringing in superb sensitivity, while their long response and recovery time as well as complex process hinder the wide application[10]. Thus, it is of great importance to develop room-temperature workable sensor materials with excellent sensing performance for next-generation sensor application.

Since the first discovery of graphene, the two dimensional (2D) structured nanomaterials have attracted extensive research interest worldwide[11–18]. Benefited from their tremendous surface-volume ratio, atomical thickness as well as excellent conducting or semiconducting property, 2D structured materials have also exhibited extraordinary potential in the gas detection field[19–22]. Specifically, their unique 2D structure exposes most atoms that could interact with environmental gas molecules and output enormous signal. Moreover, the capability of 2D nanomaterials to identify gas analytes at room temperature as well as their inherent flexible property render them to be a promising candidate for constructing flexible and wearable gas sensor integrated on a low Young's modulus substrates[23]. Even so, numerous challenges including selectivity, sensitivity, response time, recovery time, and stability have to be addressed before the practical application of 2D nanomaterials in gas detection field[24]. Taking graphene as an example, the atomic surface of graphene is chemically inert resulting in a weak adsorption of gas molecules. Strategies including surface functionalization, foreign atoms doping, defect engineering, and ligand conjugation are generally adapted to improve the sensing performance of intrinsic graphene[25, 26]. In contrast, 2D transition metal dichalcogenides (TMDCs), analogs of graphene, present multiple band structures, versatile physical and chemical properties, layer-dependent band gaps, and excellent catalytic property, that are much more adaptive in the design of practical gas sensing devices[27, 28]. However, sensor fabricated from 2D TMDCs may suffer from the sluggish response and recovery owing to the strong interaction between molecules and TMDCs surface. The incomplete recovery may gradually degrade the sensing performance and long-term stability.

Hybridizing functional elements, e.g. novel metals or metal oxides, is a feasible and controllable way to tailor the sensing performance of intrinsic 2D nanomaterials. Numerous studies have demonstrated the improvement effect of hybri-

Correspondence to: S L Zhang, slzhang@gzhu.edu.cn
Received 22 OCTOBER 2019; Revised 28 OCTOBER 2019.

dization on the gas sensing performance of 2D nanomaterials[28–30]. Gas diffusion and adsorption in 2D nanomaterials were greatly facilitated owing to the low dimensional morphologies and catalytic effect of the additive components, respectively. More recently, research interests have turned to developing graphene-like 2D/2D nanocomposites, i.e. hybridizing 2D nanomaterial with other 2D nanomaterials[31, 32]. Numerous benefits contributed by geometrical, electronic and chemical effects could be expected.

Although several recent reviews have involved in the gas sensing studies of 2D nanomaterials and 2D-based nanocomposites[33–35], no review has covered graphene-like 2D/2D nanocomposites. Herein we comprehensively review the literature of 2D/2D nanocomposites to understand the fundamental mechanisms and current progress in the field of gas detection. In this review, we summarize the reported gas sensing mechanisms of 2D nanomaterials for the basic understanding. The unique gas sensing characteristics of selected 2D/2D nanocomposites are then discussed. Lastly, the challenges and future directions to develop 2D structured nanocomposites-based sensors will be addressed. This critical review will provide great insight into the evolution of 2D structured nanocomposites to reveal the enhancement effect of hybridization.

2. Working mechanism of gas sensors

The working principle of conventional metal oxide-based gas sensors is based on the so-called surface adsorbed oxygen ions mechanism[29], while that of 2D nanomaterials-type gas sensors is mainly based on the charge-transfer processes between gas molecules and the surface of sensing materials[34]. The gas molecules act as charge acceptors or donors depending on their electron affinity upon physical or chemical adsorption on the 2D surface, resulting in the change of the overall electrical conduction. Taking MoS_2 as an example, the adsorption of oxidizing gas molecules (e.g. NO_2, SO_2, O_2, Cl_2, etc.) tend to withdraw electrons from the conduction band of MoS_2 resulting in a decreased electrical conduction, while the reducing gas molecules (e.g. NH_3, H_2, H_2S, CH_4, etc.) incline to increase the electrical conduction. Once the 2D nanomaterials are re-exposed to the air or other environmental gases, desorption of gas molecules takes place with a speed depending on the adsorption energy and diffusion condition, and the electrical conduction approach its initial value.

Gas sensors with different structures work in different ways. Here, we mainly introduce two main types of gas sensing devices including chemiresistors and field-effect transistor (FET)[36, 37]. Chemiresistors are considered to be the most commercialized sensor type due to their simplicity of fabrication and operation, high sensitivity, and long-term stability[38, 39]. In this kind of gas sensor, the sensing layer is generally deposited between two interdigitated metal electrodes on an insulating substrate. The electrical conduction property of the sensing layer would vary depending on the concentration and species of adsorbed gas. Through monitoring the resistance/current of the device before and after adsorption, the information of the target gas could be obtained. Another kind of widely used gas sensor is based on the field-effect transistor (FET)[40, 41]. In a typical FET scheme, sensing layer is deposited between two electrodes (source and drain), forming the conductive channel. A gate electrode is covered on one side of the conductive channel through a thin dielectric layer. The conductivity of channel can be modulated by a voltage applied to the gate electrode. The target gas can be detected by observing the transfer characteristics and the output characteristics of the device.

3. Features of 2D/2D nanocomposites as sensing materials

Generally, the experimental results of 2D-based sensors are often lower than their theoretical values[25]. Such discrepancy could be partially attributed to the restacking or aggregating of 2D nanosheets owing to the interlayer Van de Waals force. Thus, strategy able to prevent restacking and further improve the sensing performance should be devised. Compared to the utilization of single 2D nanomaterials, the integration of multiple 2D nanomaterials may solve several challenges of existing sensors including sensitivity, selectivity, and response (or recovery) speed issues. The collective benefits of 2D/2D hybridization can be divided into three general aspects: geometrical effects, electronic effects, and chemical effects as follows.

(1) Geometrical effects

(i) Owing to the heterogenous nature, the hybridization of different 2D nanomaterials would prevent homogeneous restacking and enlarge the active surface area.

(ii) The heterogenous hybridization would result in porous structure which exposes a large number of active sites leading to a higher sensing response, as well as facilitate the gas diffusion leading to accelerated response and recovery.

(iii) The combination of 2D nanomaterials with unique 2D structure tends to form a close contact between the components, facilitates the preservation of the intrinsic mechanical and flexible property.

(2) Electronic effects

(i) The combination of 2D nanomaterials with different semiconducting properties would form either an n/p or n/n or p/p-type heterojunction at the interface which induces heterojunction effect.

(ii) The potential energy barrier at the heterojunction hinders the electron transmission enhancing the response towards the gas with low electron affinity, and thus improving the sensor selectivity.

(iii) The heterojunction could facilitate the charge separation, avoid the charge accumulation during the adsorption/desorption process, resulting in an increased sensitivity and response speed.

(3) Chemical effects

(i) The integration of certain 2D nanomaterials with excellent catalytic properties would decrease the activation energy required in the gas adsorption/desorption process and shorten the response and recovery time.

(ii) The catalytic 2D nanomaterials could improve selective adsorption of analytes.

4. Gas sensing properties of 2D/2D nanocomposites

Motivated by these above-mentioned synergistic effects, numerous 2D/2D nanocomposites have been developed, but

Table 1. Literature study on gas sensor performance of 2D/2D nanocomposites-based gas sensors.

Material	Device type	Synthesis method	Substrate	Analyte	Limit of detection	Working temperature	Response (recovery) time	Ref
Graphene + MoS_2	Resistive	CVD + mechanical exfoliation	Polyimide	NO_2	1.2 ppm	150 °C	30 min	[45]
Graphene + MoS_2	Resistive	Liquid-phase co-exfoliation	Si/SiO_2	Methanol	10 ppm	–	210 s (220 s)	[46]
Graphene + MoS_2	Resistive	GA + ATM	Poly-Si	NO_2	50 ppb	25 °C	21.6 s (< 29.4 s)	[47]
Graphene + MoS_2	FET	CVD + mechanical exfoliation	Si/SiO_2	NO_2	1 ppm	RT	–	[48]
rGO + MoS_2	Resistive	Microwave-assisted exfoliation	PDMS	NH_3	0.48 mbar	RT	15 s	[51]
rGO + MoS_2	Resistive	Soft lithographic patterning	PET	NO_2	0.15 ppm	90 °C	–	[52]
rGO + MoS_2	Resistive	Lithography	SiO_2/Si	NO_2	2 ppm	60 °C	30 min	[53]
rGO + MoS_2	Resistive	Layer-bylayer self-assembly	SiO_2/Si	Formaldehyde	2.5 ppm	RT	73 s	[54]
rGO + MoS_2	Resistive	Self-assembly	PEN	Formaldehyde	2.5 ppm	RT	10 min (13 min)	[57]
MoS_2/WS_2	Resistive	Hydrothermal process	–	NO_2	10 ppb	RT	1.6 s (27.7 s)	[61]
rGO/WS_2	Resistive	Ball milling and sonication	Si_3N_4	NO_2	1 ppm	RT	22 min (26 min)	[56]
Defective graphene/ pristinegraphene	Current	APCVD	Ge	NO_2	1 ppm	RT	28 s (238 s)	[42]
rGO-MoS_2-CdS	Resistive	Solvothermal	–	NO_2	0.2 ppm	75 °C	25 s (34 s)	[62]
BP/h-BN/MoS_2	FET	Mechanically exfoliated + e-beam lithography	SiO_2/Si	NO_2	3.3 ppb	RT	8 min (8 min)	[63]

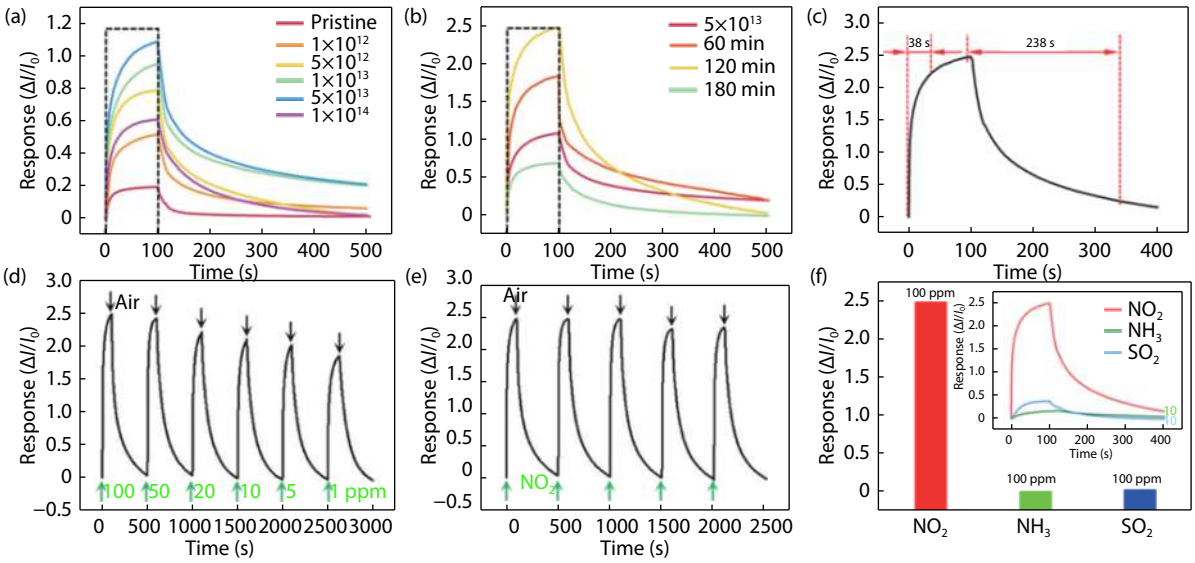

Fig. 1. (Color online) The sensing response of DGr/Gr hybrid fabricated with different (a) irradiation fluence and (b) H_2 etching time to 100 ppm NO_2 at room temperature. (c) The response-recovery curve of the gas sensor based on DGr/Gr. (d) Dynamic response of the DGr/Gr based sensor to different concentrations of NO_2 at room temperature. (e) Cycled response to 100 ppm NO_2 at room temperature. (f) Responses of the DGr/Gr based gas sensor toward different gas species at room temperature[34].

not many works have been done regarding gas sensing properties of 2D/2D nanocomposites as summarized in Table 1. In this section, we introduce the recent progress on the graphene-like 2D/2D nanocomposites-based gas sensors. Relative works involving different substrates including flexible polymer and rigid silica as well as different working temperatures ranging from room temperature (RT) to 150 °C have been included for a comprehensive understanding of the recent trend. The cases have been classified with hybrid types, since the mechanism and gas sensing performance of 2D/2D nanocomposites are ineluctably influenced by the choice of material with their innate properties.

4.1. Graphene + graphene

Ma *et al.* fabricated a gas sensor based on defective graphene (DGr)/pristine graphene (Gr) hybrid layer[42]. The defect density of defective graphene was controlled by the fluence of Si^+ implantation, and the defect size was tuned by an H_2 etching process. The defective graphene was transferred onto pristine graphene with a PMMA assisted wet trans-

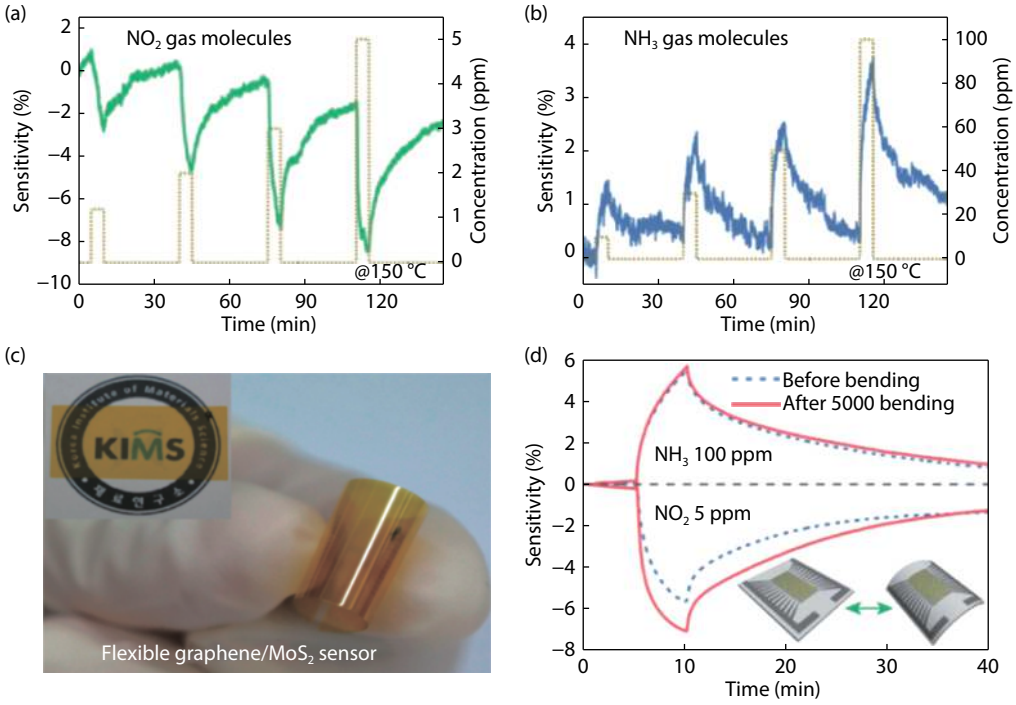

Fig. 2. (Color online) (a) Transient response of graphene/MoS_2 sensor to NO_2 gas molecules (1.2 to 5 ppm). (b) Transient response of graphene/MoS_2 sensor to NH_3 gas molecules (5 to 100 ppm). All gas-sensing tests were performed at an operating temperature of 150 °C. (c) Optical image of a graphene/MoS_2 heterostructured device on a bent polyimide substrate, inset displays the semitransparent sensing device placed on a paper with the KIMS logo. (d) Comparison of the gas response characteristics of the flexible heterostructured device before/after the bending cycle test, inset is the 3D schematic images showing the bending test condition. No serious performance degradation was observed, even after performing 5000 bending cycle tests[45].

fer method to finally obtain Gr/DGr hybrid-based gas sensor device. As shown in Figs. 1(a)–1(c), both the defect density and defect size could influence the response performance significantly. The DGr prepared with a 5×10^{13} cm^{-2} Si^+ ion bombardment and 120 min H_2 etching exhibited the best sensing performance with a maximum response value over 248% at room temperature. The dynamic response and reproducibility properties as shown in Figs. 1(d) and 1(e), respectively, indicated the excellent sensing performance of DGr/Gr hybrid. Furthermore, the defect engineering endows the Gr strong adsorption with NO_2 gas molecules. As shown in Fig. 1(f), the typical response of DGr/Gr hybrid to NO_2 was at least 65 times higher than that to the other target gases, indicating that the excellent selectivity property of DGr/Gr based gas sensor.

4.2. Graphene + MoS_2

The recent studies on the integration of graphene with 2D layered semiconductors have emerged for different application, in which the graphene/MoS_2 nanocomposites have been researched mostly[43, 44]. In this combination, the graphene usually plays the role of conductive layer, and the MoS_2 acts as the analyte acceptor. Cho *et al.* reported an atomically thin graphene/MoS_2 heterostructure-based gas sensor, where the patterned graphene as electrodes was synthesized via chemical vapor deposition (CVD) and MoS_2 was mechanically exfoliated[45]. As shown in Figs. 2(a) and 2(b), the limit detection concentration of this device was as low as 1.2 ppm for NO_2 gas and 5 ppm for NH_3 at 150 °C. Furthermore, the device can be constructed on a polyimide substrate and the gas response characteristic of the flexible device was well maintained at 150 °C, even after 5000 bending cycle tests, as displayed in Figs. 2(c) and 2(d). Zhang *et al.* fabricated graphene/MoS_2 nanocomposite through a liquid-phase co-exfoliation method and constructed a thin film gas sensor for methanol detection[46]. On the interface of the exfoliated graphene and MoS_2, the MoS_2 acts as an electron donor which results in a slight n-type doping effect to graphene. The methanol as a typical reducing gas enhanced the n-type doping level of MoS_2, as shown in Figs. 3(a) and 3(b). Results showed that the sensitivity of graphene/MoS_2 nanocomposite gas sensor was almost double to that of pure MoS_2 sensor. The response time and recovery time were also shortened. The remarkable improvement of sensing performance was ascribed to the synergetic effect of graphene and MoS_2 nanoflakes, in which MoS_2 acted as an excellent analytes acceptor and graphene acted as a charge highway, as shown in Fig. 3(c). The graphene/MoS_2 nanocomposite sensor also presented excellent stability (Fig. 3(d)).

Performance improvement of 2D gas sensor can also be realized by ingenious structure design. Through synthesizing MoS_2/graphene hybrid aerogel (GA), Long *et al.* integrated the novel 3D hybrid aerogel on a low power microheater platform, realizing an excellent NO_2 detection device[47]. As seen in Figs. 4(a) and 4(b), the limit of detection toward NO_2 was below 50 ppb (14 ppb) at room temperature (200 °C). The average time of response and recovery was 21.6 s and 29.4 s at 200 °C against different NO_2 concentrations, from 50 ppb to 1 ppm (Fig. 4(c)). Fig. 4(d) was a plot of the selectivity of the MoS_2/GA sensor compared to GA alone at 200 °C, and the MoS_2/GA sensor exhibited excellent selectivity than GA

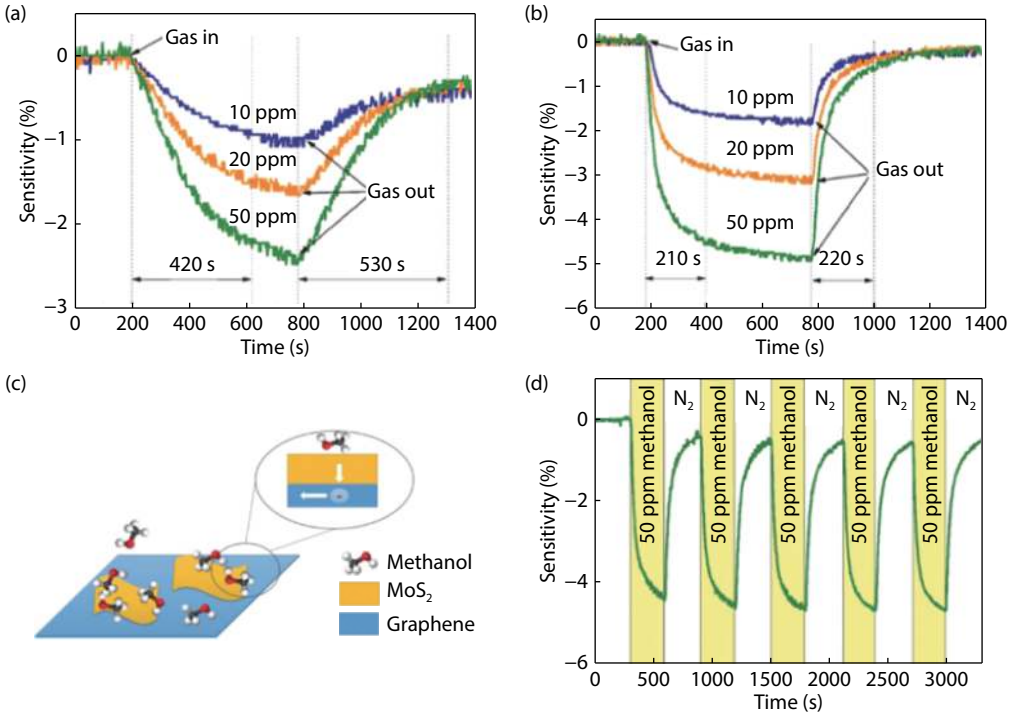

Fig. 3. (Color online) Typical sensing response of (a) the exfoliated MoS_2 based thin film sensor and (b) the co-exfoliated MoS_2/graphene-based thin film sensor to 10, 20, and 50 ppm methanol. (c) The synergetic effect of the MoS_2/graphene nanocomposite as methanol gas sensor. (d) Repeated sensing response of the co-exfoliated MoS_2/graphene thin film sensor to 50 ppm methanol[46].

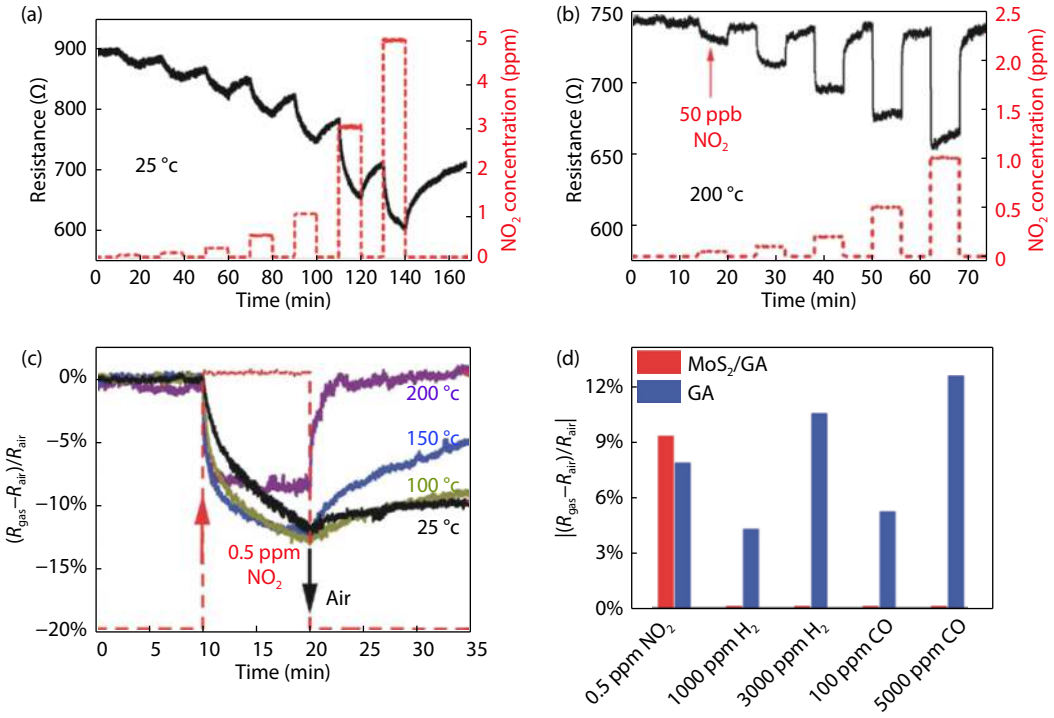

Fig. 4. (Color online) (a) Real time response of the MoS_2/graphene hybrid aerogel (MGA) sensor at room temperature toward different NO_2 concentrations. (b) Real time resistance change of the MGA sensor with the microheater temperature of 200 °C. (c) MGA sensor response to 0.5 ppm NO_2 at various microheater temperatures, displaying improvement in response and recovery time. (d) Selectivity peroperties of the MGA sensor compared to that of GA alone at microheater temperature of 200 °C[47].

sensor. The good NO_2 detection performance was attributed to a novel structure of 3D hybrid aerogel, in which the high electrical and thermal conductivity graphene serves as a scaffold, and single to few-layer MoS_2 covered on the scaffold serving as selective and sensitive layer for NO_2 detection. Meanwhile, the 3D graphene scaffold provided the high specific area, which availed the carrier transport. Hiroshi Tabata *et al.* investigated the NO_2 sensing characteristics of a graphene/MoS_2 heterojunction (GMH) utilizing a passivation technique with gas barrier layers[48]. As shown in Figs. 5(a) and 5(b), the passivation technique guaranteed the response was originated from the GMH area. For the 2D layered semi-

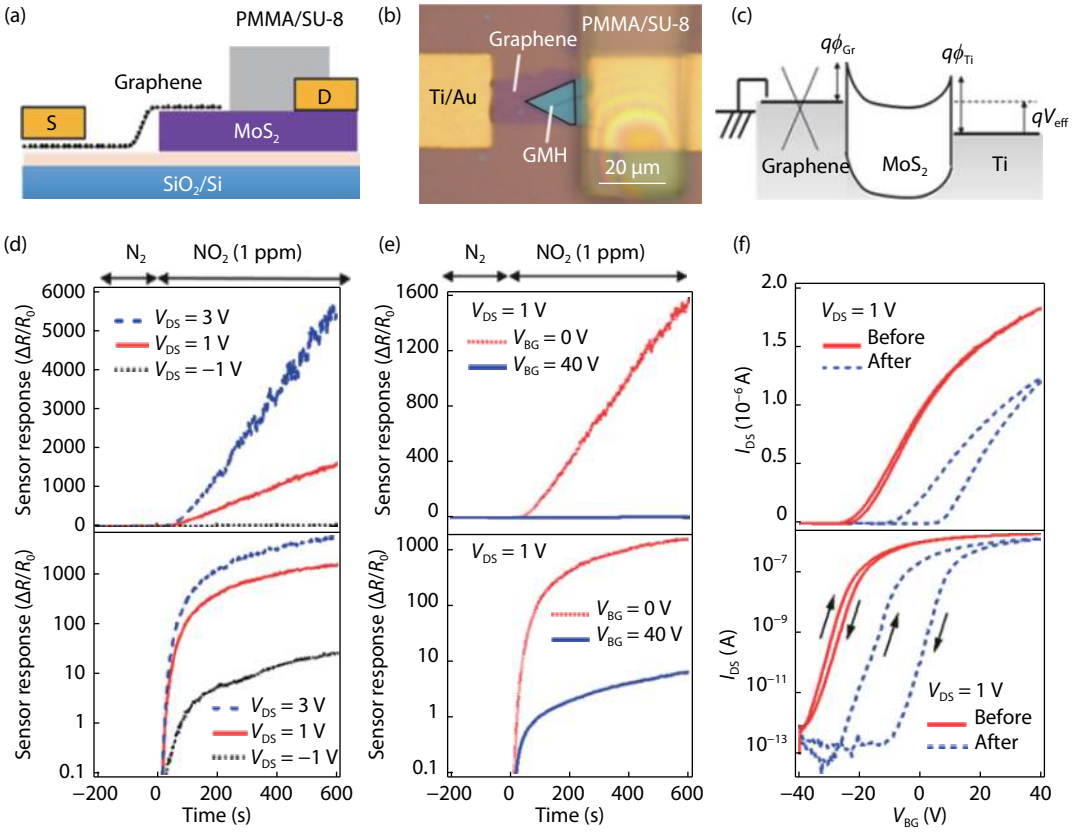

Fig. 5. (Color online) (a) Schematic and (b) optical microscope images of the graphene/MoS_2 heterojunction (GMH) device with a gas barrier layer. (c) Metal–semiconductor–metal diode model for n-type MoS_2 with graphene and Ti asymmetric contacts and its band diagram. (d) Time-dependent sensor responses of GMH under different bias conditions (V_{DS} = −1, 1, and 3 V) in linear scale (top) and semilogarithmic scale (bottom). (e) Time-dependent sensor responses of GMH under different gate voltages (V_{BG} = 0 and 40 V) in linear scale (top) and semilogarithmic scale (bottom). (f) Transfer curves of the GMH device measured at V_{DS} = 1 V in linear (top) and in semilogarithmic scales (bottom)[48].

conductors rarely have the dangling bonds on their surface, the graphene/MoS_2 interface has a weaker Fermi-level pinning effect (Fig. 5(c)), which enabled more effective modulation of the Schottky barrier height in the graphene/MoS_2 interface. The GMH device demonstrated a significant change in resistance, by a factor of greater than 10^3, upon exposure to 1 ppm NO_2 under a reverse-bias condition, while it dramatically decreased when measured at a large forward bias, as displayed in Fig. 5(d). Fig. 5(e) plotted the time-dependent sensor responses of GMH under different gate voltages. Fig. 5(f) displayed the corresponding drain current against drain voltage curves before and after NO_2 exposure. It was found when a reverse bias or a large negative back-gate voltage was applied, the sensor responded over 10^3 upon exposure to 1 ppm NO_2. This is because the drain current was determined by the NO_2-induced modulation in the GMH and the barrier height at the counter Schottky diode of the MoS_2/Ti contact was not reflected in the sensor response in both cases. Conversely, the response was decreased due to the fact that the barrier height at the counter Schottky diode of the MoS_2/Ti contact covered the response of NO_2-induced modulation.

4.3. rGO + MoS_2

In case of sensor application, reduced graphene oxide (rGO) presents superiority compared to intrinsic graphene and graphene oxide (GO) on the account of its rich functional groups and partly regained conductivity[49]. Sun *et al.* synthesized rGO/MoS_2 composites by a hydrothermal method, using 2D rGO as template[50]. The effect of the ratio of MoS_2 in rGO/MoS_2 composites for sensing hydrogen peroxide (H_2O_2) vapor was studied. The average response and response/recovery time towards 50 ppm of H_2O_2, C_3H_6O, C_2H_6O vapors at room temperature were shown in Figs. 6(a)–6(c). Results show that rGO/MoS_2 composites gas sensors had excellent selectivity toward H_2O_2 and the response/recovery time were both less than 20 s. Comparing with pure rGO sensor, the response toward H_2O_2 vapor achieved an increase of about 12 times. Kumar and his co-workers synthesized rGO/MoS_2 hybrid material with microwave-assistant method to fabricate gas sensor on polymer substrate[51]. The effect of thickness of sensitive layer on sensing performance had been investigated. Results show that the rGO/MoS_2 layer had the best response toward NH_3 and lowest sensitivity towards N_2. When the thickness of rGO/MoS_2 layer was 2 mm, the ratio of response between NH_3 and N_2 differed three orders of magnitude. The response of the 10 μm thickness rGO/MoS_2 layer was about two orders of magnitude higher than that of the 2 mm thickness layer, indicating that only the top layer effectively attended the reaction with the gas molecules. Jung *et al.* fabricated highly transparent and flexible NO_2 gas sensor film based on MoS_2/rGO composites through soft lithographic patterning method[52]. The transmittance of the thin film MoS_2/rGO composites gas sensor on PET substrate reached 93% and the sensing characteristics were still maintained

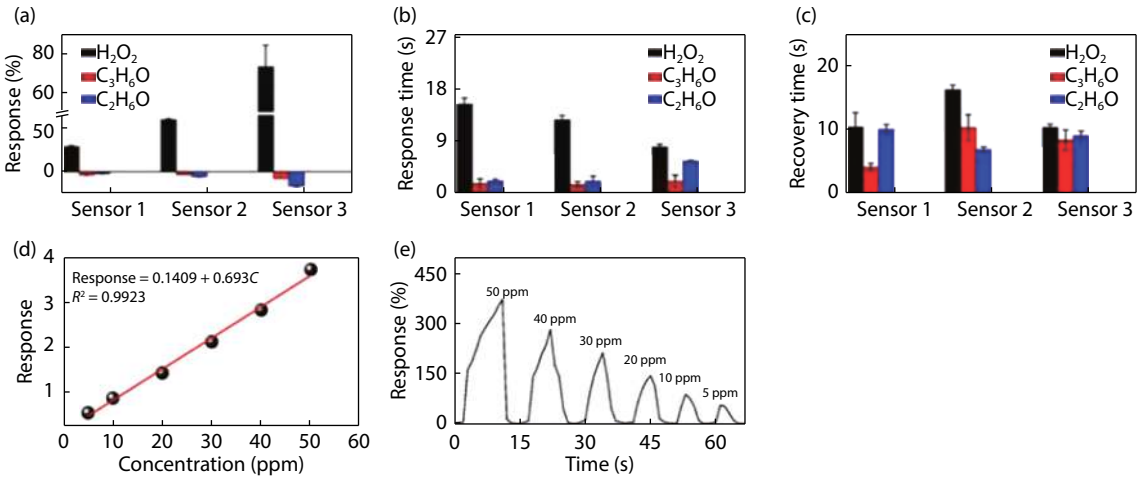

Fig. 6. (Color online) Statistical graph of (a) average response, (b) response time and (c) recovery time of rGO/MoS_2 composites gas sensors. (d) Plots of the fitting of response vs. concentration. (e) Dynamic response of MoS_2/rGO sensor to different concentrations of H_2O_2 vapor[50].

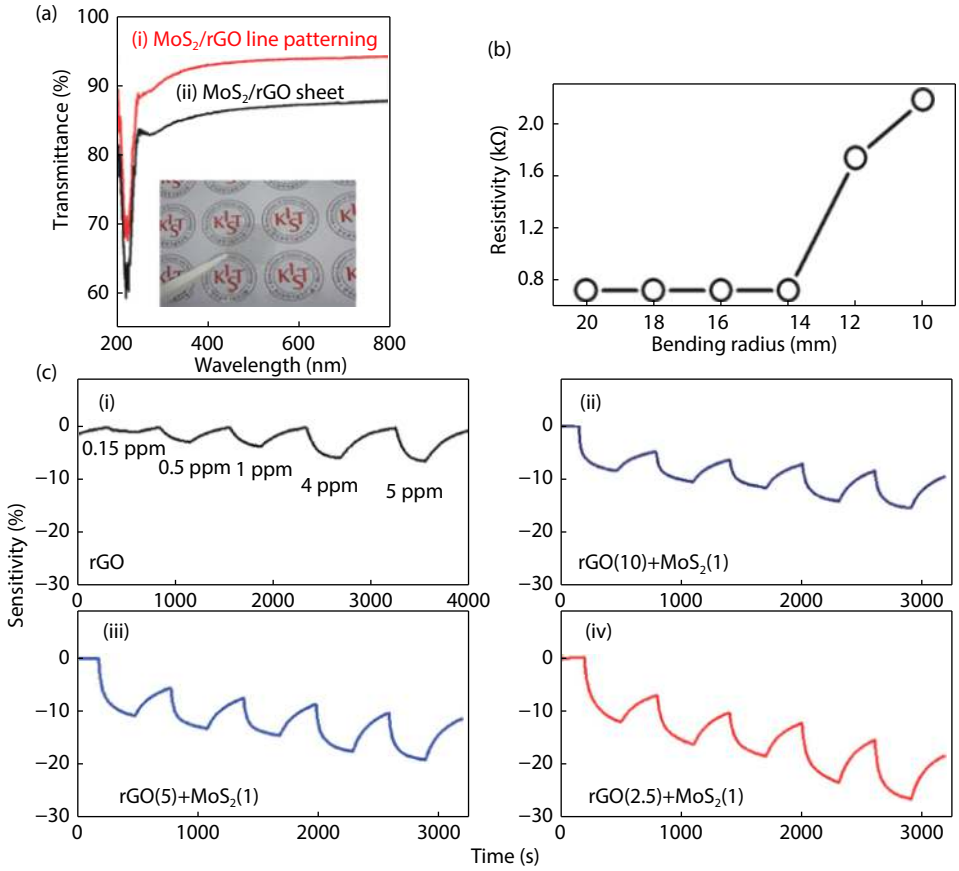

Fig. 7. (Color online) (a) The UV–vis transmittance spectra of patterned MoS_2/rGO layer. (b) Resistivity of the MoS_2/rGO layer on PET as the function of bending radius. (c) Dynamic response of (i) rGO, (ii) MoS_2/rGO (1 : 10), (iii) MoS_2/rGO (1 : 5) and (iv) MoS_2/rGO (1 : 2.5) thin film gas sensor with different concentrations of NO_2[52].

with a bending radius of 14 mm as shown in Figs. 7(a) and 7(b). Moreover, the transparent and flexible gas sensor could detect a concentration as low as 0.15 ppm of NO_2. The sensitivity of the MoS_2/rGO composites thin film gas sensor was four times higher than that of pure rGO thin gas sensor under a bias voltage of 0.1 V at 90 °C. The sensing response also showed a composition dependent property as shown in Fig. 7(c). Results revealed that the MoS_2/rGO composite with a ratio of 1 : 2.5 presented the best response toward NO_2 which was four times higher than that of pure rGO gas sensor.

Zhou *et al.* prepared MoS_2/rGO composite films by a combination of hydrothermal method and air brush technology and investigated their NO_2 sensing response at 60 °C[53]. Fig. 8 shows the sensing performance of pure rGO sensor and MoS_2/rGO composite sensor, and both sensors exhibited p-type characters. As shown in Figs. 8(a) and 8(b), rGO/MoS_2 composite sensor exhibited a sensing response towards 2 ppm NO_2 approximately twofold to that of pure rGO sensor. Figs. 8(d)–8(f) depicted the *I*–*V* characteristics of rGO-Au, MoS_2-Au and rGO/MoS_2-Au contacts, respectively. An ohm-

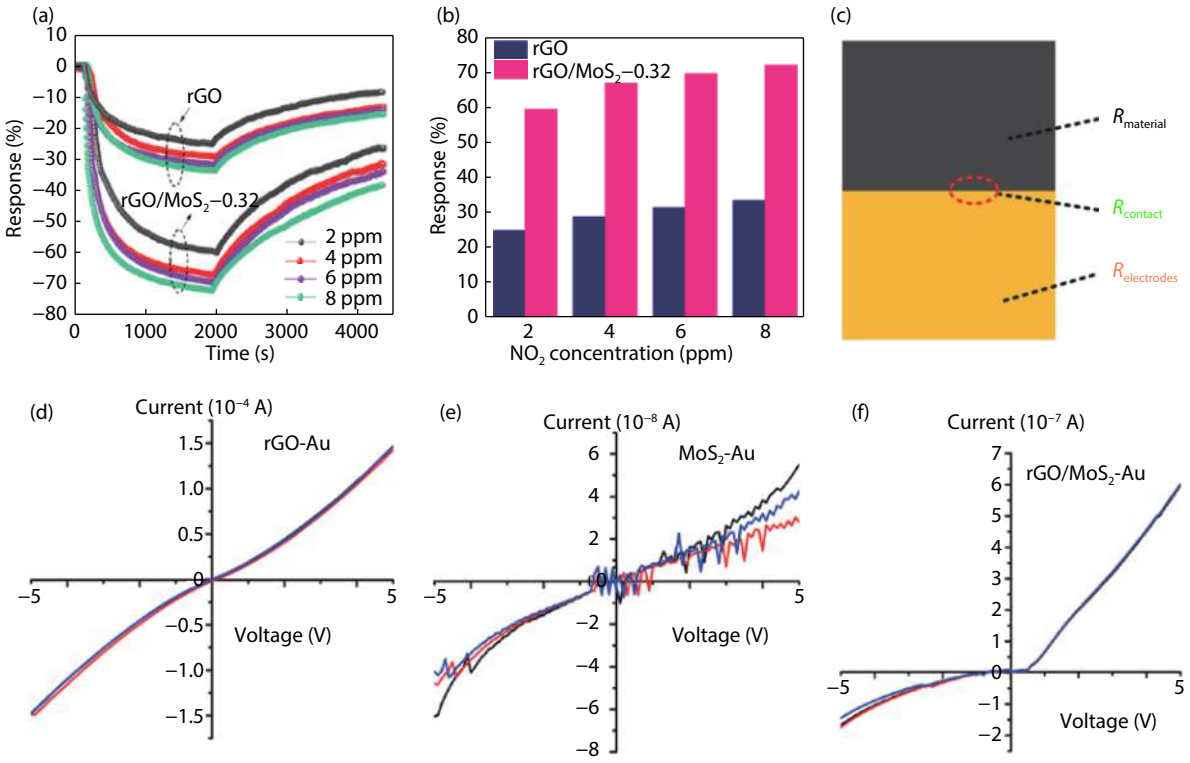

Fig. 8. (Color online) (a) Sensing responses of rGO sensor and rGO/MoS_2 sensor toward various concentrations of NO_2. (b) Histogram analysis obtained from (a). (c) Schematic illustration of resistance configuration of interdigital electrode sensors. *I*–*V* relationships of (d) rGO-Au, (e) MoS_2-Au and (f) rGO/MoS_2-Au contacts[53].

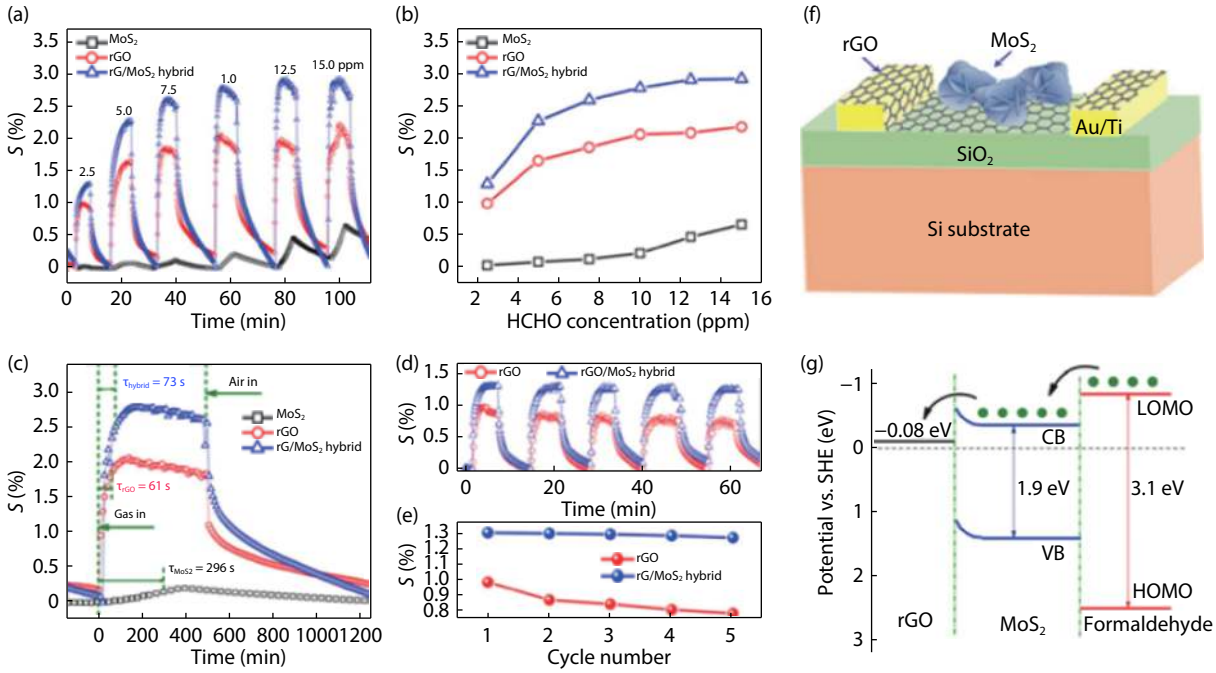

Fig. 9. (Color online) (a) Dynamic response curves and (b) summarized response values of the devices based on MoS_2, rGO and rGO/MoS_2 hybrids film toward HCHO at room temperature. (c) Comparison of the response time of the three devices to HCHO. (d) Reproducibility and (e) stability properties of the rGO and rGO/MoS_2 hybrid films toward 2.5 ppm HCHO. Schematic illustrations of (f) the fabricated sensing device and (g) the energy diagram of rGO, MoS_2 and formaldehyde[54].

ic contact was observed for rGO-Au, MoS_2-Au contacts. With respect to the rGO/MoS_2-Au contact, obvious rectifying behavior was observed indicating the existence of p–n junctions at interface of rGO and MoS_2. The surface-absorbed NO_2 withdrew electrons from both rGO and MoS_2 and extended the hole accumulation region (HAR) on rGO surface and electron-shell depletion region (EDR) on MoS_2 surface. As the resistance change of MoS_2 was more reluctant than that of rGO, the HAR extension exerted more effect on total resistance alteration than EDR, which led to the resistance decreased. Li *et*

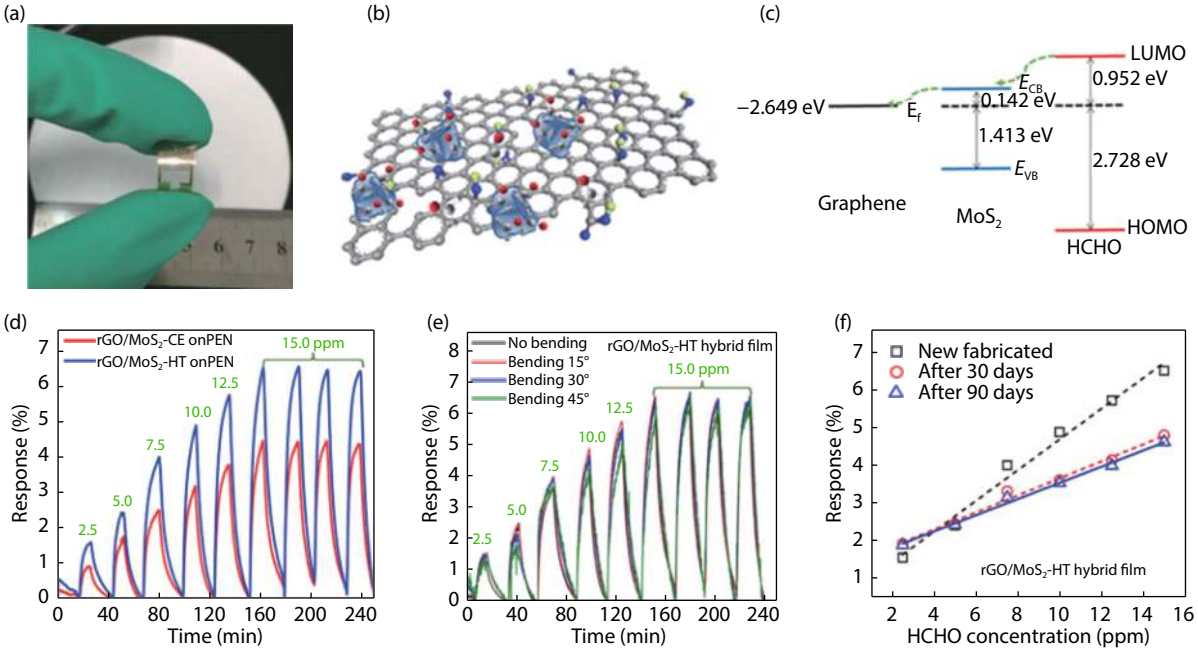

Fig. 10. (Color online) (a) Photo image of the flexible device based on rGO/MoS_2 hybrid film in the bending state. (b) Adsorption model of HCHO molecule on rGO/MoS_2 hybrid film. (c) Schematic illustration of HCHO sensing mechanism of rGO/MoS_2 hybrid film. (d) Real-time sensing response curves of the rGO/MoS_2-HT and rGO/MoS_2-CE sensors to 2.5–15 ppm HCHO. (e) Real-time sensing response curves of the rGO/MoS_2-HT sensor to 2.5–15 ppm HCHO upon different bending angles. (f) Long-term stability of rGO/MoS_2-HT sensor[57].

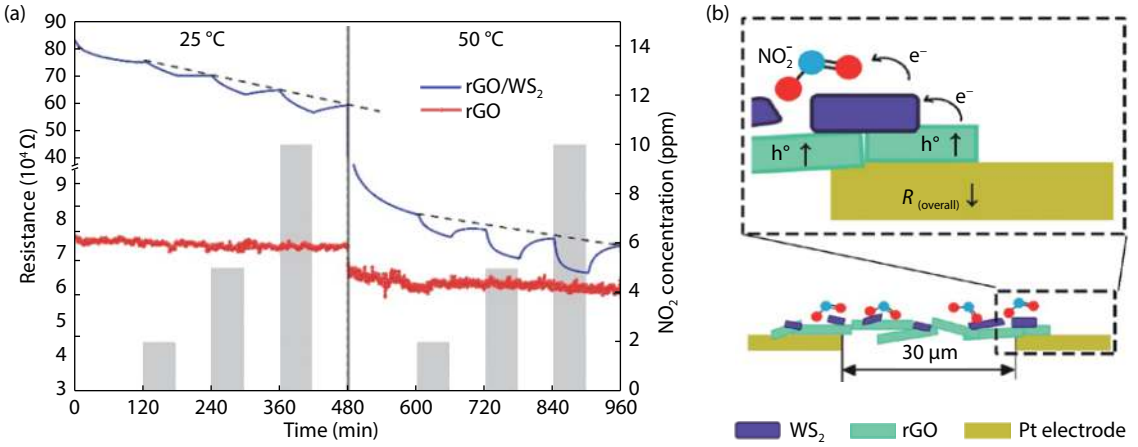

Fig. 11. (Color online) (a) Sensing responses of single rGO (red line) and WS_2-decorated rGO films (blue line) in dry air and 2–10 ppm NO_2 operated at (left) 25 °C and (right) 50 °C. (b) Schematic illustration of the proposed sensing mechanism of WS_2-decorated rGO hybrid upon NO_2 exposure[56].

al. fabricated a hybrid film composed of rGO and MoS_2 for formaldehyde detection by a simple layer-by-layer self-assembly method[54]. The rGO/MoS_2 hybrid film exhibit fast response/recovery and high reproducibility than that of the MoS_2 film as shown in Figs. 9(a)–9(f). The enhanced sensing performance can be illustrated with Fig. 8(g), electrons donated by formaldehyde firstly transferred to conduction band of MoS_2 mediated by the surface adsorbed oxygen, then further transferred to the rGO substrate, leading to fast conductive change of the hybrid films. Such a two-step efficient electron transfer could enhance the electron transfer from analytes to rGO, thereby increasing the sensitivity of the hybrid films[55, 56].

In another work, authors fabricated rGO/MoS_2 hybrid films on flexible polyethylene naphthalate (PEN) substrates by a simple self-assembly method and studied their sensing performance towards 2.5–15 ppm HCHO at room temperature (Fig. 10(a))[57]. Two kinds of MoS_2 were prepared by either hydrothermal synthesis (HT) or chemical exfoliation (CE) method. The results revealed that the surface defects on MoS_2 enhanced the sensitivity of rGO/MoS_2 sensor, for the MoS_2 produced by HT process had more defects than that of CE method. Moreover, Fig. 10(e) shows the bending property of rGO/MoS_2-HT sensor. Only small decline of sensing response was observed suggesting the robustness of the flexible devices. The authors believed that the rGO in the rGO/MoS_2 composite film acted as a conductive network that bridges the electrodes and the continuous conducting channel resulting in a robust bending resistive sensing layer. The result of density functional theory calculation, as depicted in Fig. 10(c), shows that the MoS_2 nanosheets in the hybrid film acted as HCHO adsorbent and electron acceptors while the rGO

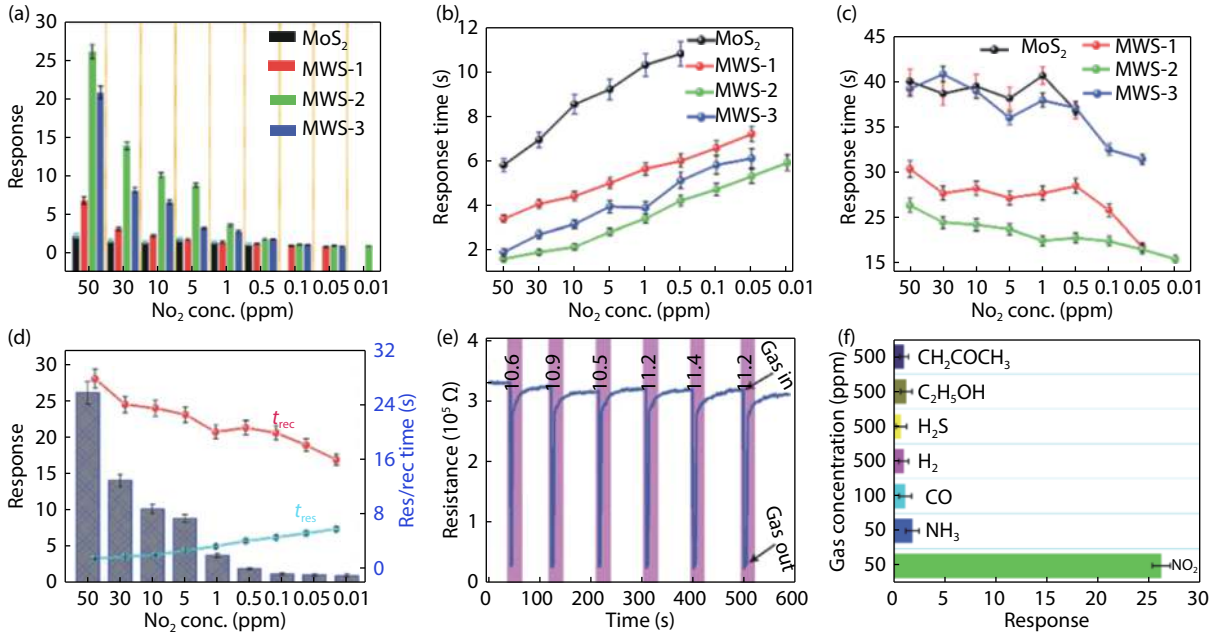

Fig. 12. (Color online) (a) Response of four types of MoS_2/WS_2 heterojunction toward different concentrations of NO_2 at room temperature. (b and c) Response time and recovery time of the sensors, respectively. (d) Response, and response/recovery time of optimized MoS_2/WS_2 heterojunction as the functions of gas concentrations. (e) Reproducibility of MoS_2/WS_2 heterojunction sensor toward 10 ppm NO_2 at room temperature. (f) Selective response of MoS_2/WS_2 heterojunction sensor[61].

served as a conducting network, and thus resulted in a p-type response. The introduction of MoS_2 enhanced the adsorption of HCHO molecules[58] and decreased the energy barriers in electron transfer process[59, 60].

4.4. rGO + other TMDCs

Paolucci *et al.* reported a NO_2 gas sensor fabricated from WS_2-decorated rGO composite[56]. Fig. 11 shows the responses of a single rGO film and a WS_2-decorated rGO film to dry air at 25 and 50 °C. The substantial contribution of the WS_2 semiconductor to the overall resistance response was confirmed by comparing the baseline values. The elevated operating temperature at 50 °C resulted in an enhanced response. However, the drift of resistance baseline indicated the serious drawback of WS_2 decorated rGO hybrid as gas sensor material. Fig. 11(b) presents a schematic illustration of the sensing model of WS_2-decorated rGO film, in which NO_2 as electron acceptor captured electrons form n-type WS_2 surface. As a consequence, electron-depleted n-type WS_2 flakes drained electrons from the underlying p-type rGO resulting in the increase of hole concentration in p-type rGO and decrease of the overall resistance of the p-type WS_2-decorated rGO. The rapid electron transport from the highly conducting rGO to the less-conducting WS_2 contributed much to the final sensing performance in which the rGO flakes serve as highly conductive channels bridging the distant electrodes.

4.5. TMDCs + TMDCs

The integration of multiple TMDCs is also a favorable way to improve the sensing performance of the single TMDCs since their rich semiconducting and chemical catalytic properties make it possible to form numerous distinct functional heterostructure. Ikram *et al.* synthesized a heterojunction of few-layer MoS_2 with multilayer WS_2 via a simple one-pot hydrothermal process[61]. The atomic ratio of Mo and W was well controlled and a series of MoS_2/WS_2 heterostructures were synthesized. Figs. 12(a)–12(c) show the response value and response/recovery time of those MoS_2/WS_2 heterostructure sensors upon exposure to 0.01–50 ppm NO_2. The results show there was an optimized atomic ratio of Mo and W which exhibits best response, quickest response/recovery time and lowest detection limit. The optimized heterostructure sensor exhibited very quick response (6 s) and recovery (16 s) at room temperature (Figs. 12(b)) and 12(c)). The MoS_2/WS_2 heterostructure sensors presented p-type sensing behavior as the resistance of the sensor decreased abruptly upon exposure to NO_2, as shown in Fig. 12(e). Impressively, the MoS_2/WS_2 heterostructure sensor with optimized composition achieved the lowest detection limit of 0.01 ppm, much lower than that of pure MoS_2 (Fig. 12(d)). Figs. 12(e) and 12(f) demonstrated the excellent reproducibility and high selectivity of the MoS_2/WS_2 heterojunction based NO_2 sensor. This work suggests that the integration of two TMDCs could not only improve the sensing response but also address the mail challenges existing in single TMDC-based gas sensor, i.e. slow response speed and low selectivity. Sun *et al.*[55] had studied the geometry, electronic structures, and electron transport properties of the MoS_2/WS_2 heterojunction with first principles calculations. The adsorption of CO, H_2O, NH_3, NO, and NO_2 gas molecules on the MoS_2/WS_2 heterojunction had also been studied. Results show that NH_3 performed as electron donor and all other gases performed as electron acceptor. The gas molecule adsorption significantly affected the electronic transport properties of the heterojunction. Both the rectification behavior and the value of the passing current can be altered by gas adsorption.

4.6. Ternary 2D nanocomposites

Previously we discussed the merits of binary 2D/2D nanocomposites as gas sensor material. Recent studies show that

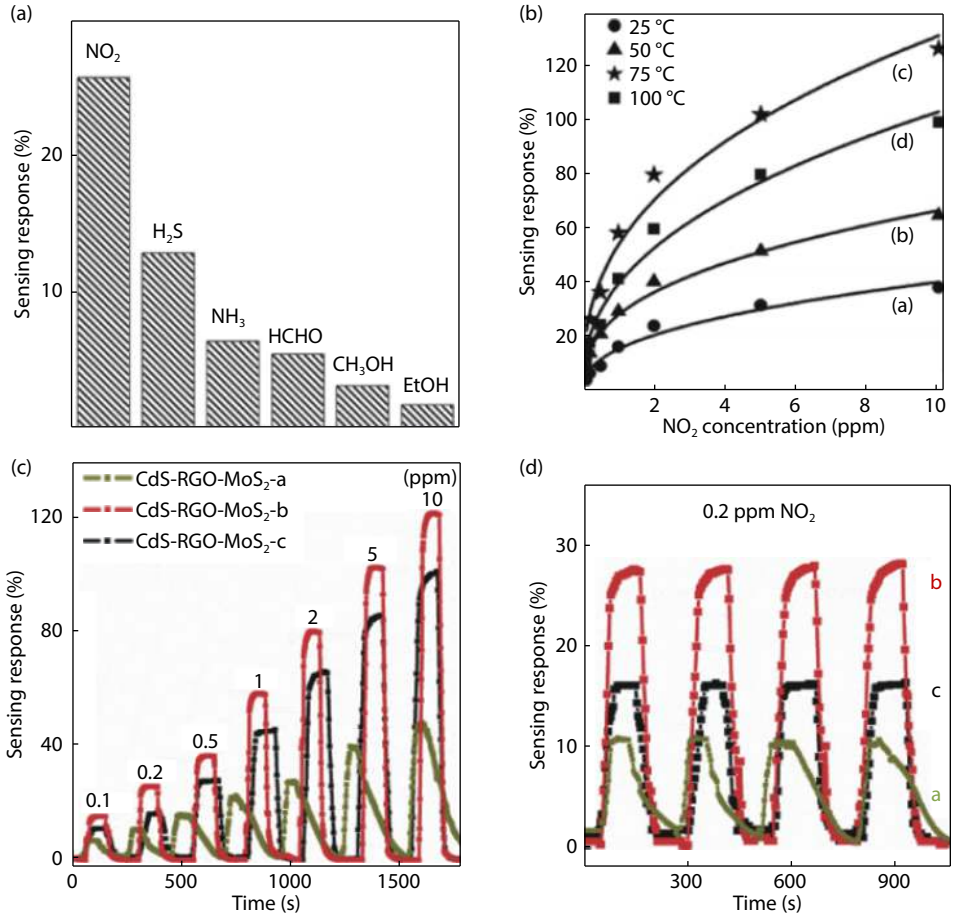

Fig. 13. (Color online) (a) Sensing response values of rGO-MoS_2-CdS nanocomposite film to 0.2 ppm of different target gases at 75 °C. (b) Normalized responses of rGO-MoS_2-CdS nanocomposite gas sensor as a function of NO_2 gas concentrations under different operation temperatures: (a) 25 °C, (b) 50 °C, (c) 75 °C, and (d) 100 °C. (c) Dynamic responses of three types of rGO-MoS_2-CdS nanocomposite sensors toward different concentration of NO_2 at 75 °C. (d) Cyclic response of three types of rGO-MoS_2-CdS nanocomposite sensors toward 0.2 ppm of NO_2[62].

the sensing property of binary 2D/2D nanocomposites could be further enhanced by adding the third component, i.e. the ternary 2D/2D nanocomposites. Shao *et al.* found that CdS nanocones could be grown on the 2D layered rGO-MoS_2 substrate by a facile solvothermal treatment process, to form rGO-MoS_2-CdS nanocomposite films[62]. As shown in Fig. 13, the gas sensor based on rGO-MoS_2-CdS films, with the higher specific surface area, more adsorption sites and lots of heterojunctions, showed a largely enhanced sensor response of 27.4% toward 0.2 ppm NO_2, about 7 times higher than the value of binary rGO-MoS_2 2D nanocomposite based gas sensor. Moreover, the gas sensor presented an outstanding selectivity toward NO_2 gas against the other gases.

Other than the chemical integration, the 2D nanomaterials could also be geometrically integrated to form a functional device. Sigang Shi *et al.* reported a gas sensor based on a ternary 2D nanomaterial-based FET device in which few-layer black phosphorus (BP), boron nitride (BN) and molybdenum disulfide (MoS_2) were used as the top-gate, dielectric layer and conduction channel, respectively[63]. Fig. 14(a) displays the device configuration where the top-gate of BP with a superior gas adsorption capability serves as the sensing material, while the conduction channel of MoS_2 is isolated from ambient environment by the coverage of the BN dielectric layer. The adsorption of the gas analyte on the gate material led to the charge transfer from the gas analyte to the gate material, which modulated the Fermi level of both the gate and conduction channel materials, and thus the resistance of the conduction channel. Figs. 14(b) and 14(c) plot the band structure of the 2D material FET before and after NO_2 adsorption. When the device was exposed to the NO_2 gas, the Fermi level of p-doped BP shifted towards the valence band, leading to the shift of MoS_2 towards the valence band. The movement of Fermi level of MoS_2 resulting in the increase of channel resistance at fixed gated and source-drain biases. The kinetic information of gas adsorption on the device was then able to obtain. Fig. 14(f) shows the real-time response of the device to NO_2 with concentrations ranging from 10–100 ppb. The device failed to fully recover back to the baseline upon in N_2 for 15 min, which may be due to the strong adsorption energy between BP and NO_2. The sensitivity of the ternary 2D FET device for NO_2 achieved 1.19% resistance change per ppb, and the detection limit to NO_2 was 3.3 ppb. As shown in Figs. 14(g)–14(i), FET device was also tested with NH_3 and various volatile organic compounds. The device resistance increased upon exposure to DCM, while decreasing upon exposure to NH_3, hexane, acetone and DMF.

5. Conclusions and outlook

In this review, we comprehensively summarize the achievements in recent studies on the gas sensor application of 2D/2D nanocomposites. The sensing mechanism of 2D nano-

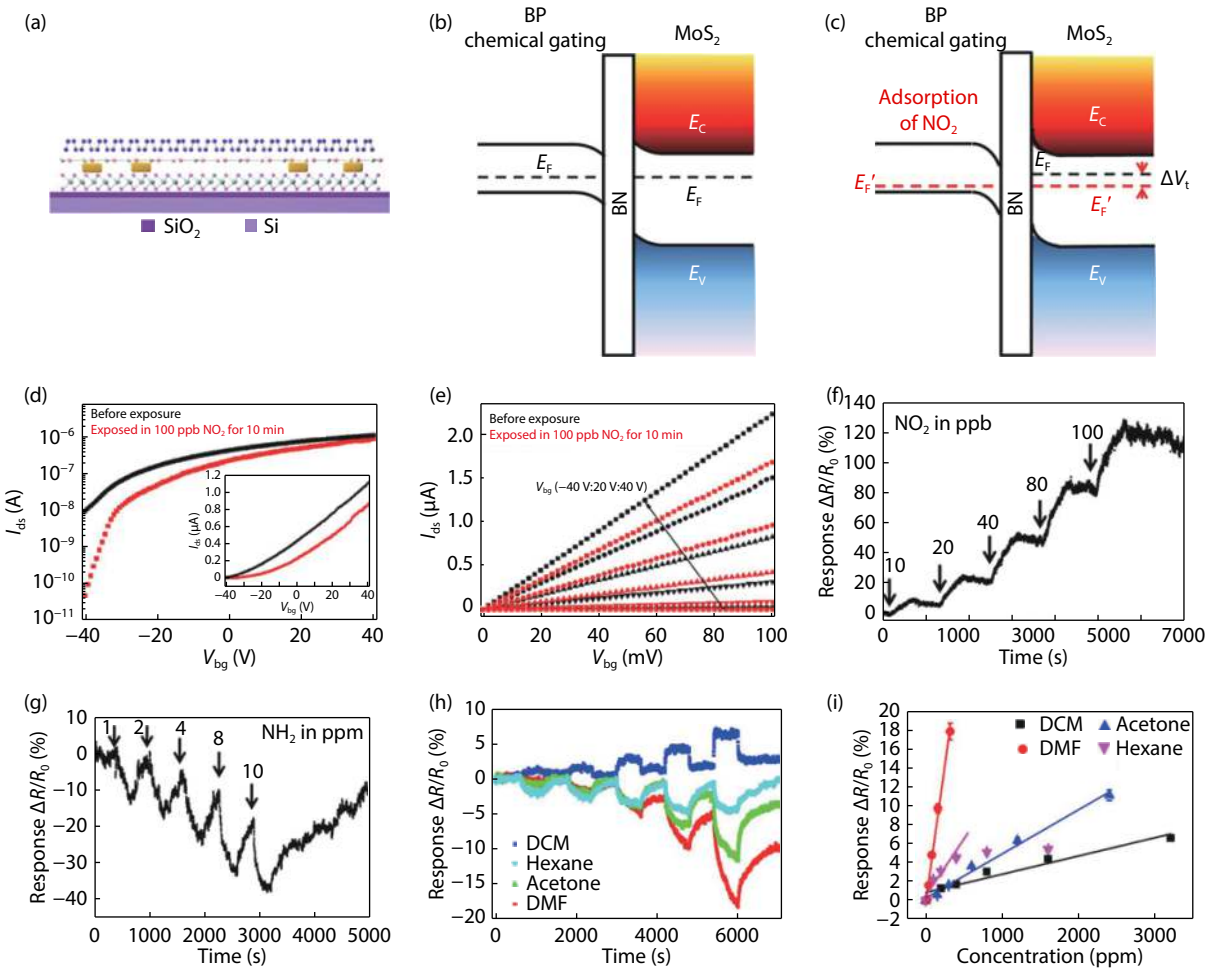

Fig. 14. (Color online) (a) Schematic of the ternary 2D nanomaterial-based FET device. (b) Band structure of the FET device before and (c) after NO_2 adsorption. (d) Transfer and (e) output curves of the FET before and after exposure to 100 ppb NO_2 for 10 min. (f) Real-time sensing response of the FET to NO_2. (g) Real-time sensing response of the FET device to NH_3. (h) Real-time sensing response of the FET device to DCM, hexane, acetone and DMF. (i) Relative resistance change as a function of the square root of the gas concentrations[63].

materials was briefly introduced. The collective benefits and mechanisms of 2D/2D nanocomposites were discussed in three aspects: geometrical effects, electronic effects, and chemical effects. The reported experimental results demonstrated the promising gas sensor performances, such as high sensitivity and selectivity, improved response and recovery speed, and long-term stability of 2D/2D nanocomposites-based sensors even at room temperature. Part of the sensor devices were fabricated on polymer substrates presenting excellent flexible property. Such achievements offer great potential for practical implementation as next-generation flexible and wearable gas sensors.

Although significant progress has been demonstrated, there are still remaining questions as follows:

(1) The sensing mechanism of single 2D nanomaterials has been developed much, while the underlying sensing mechanisms of 2D/2D nanocomposites are still vague. The role of synergistic effect and hybridized effect on gas sensing performance of 2D/2D nanocomposites should be determined.

(2) Several teams reported the improved selectivity after hybridizing different 2D nanomaterials. However, scientific comprehension on such improvement has not been achieved. More simulation works and experimental results are required to clarify this issue.

(3) Most of the reported literatures in this field have not involved in the effect of humidity on the sensing performance of 2D/2D nanocomposites, while recent works have found numerous 2D TMDCs are very sensitive to water molecules. Thus the cross influence of humidity and target gases should be carefully investigated.

(4) Numerous studies have shown that the sensing performance of 2D/2D nanocomposites are greatly dependent on the ratio of the components. Considering the complexity and economy, however, current researches on 2D/2D nanocomposites generally involved in several compositions. Systematical study on the optimization of the composition ratio is required.

In terms of future prospective, we believe that there are still tremendous opportunities in the field of 2D/2D nanocomposites-based gas sensors. Our comment on the future development trends of 2D/2D nanocomposites-based gas sensors could be divided into three sections. First, hundreds of new semiconducting 2D nanomaterials have been discovered in last decade. These analogs of graphene presenting distinct electronic and chemical properties with tremendous specific surface are ideal materials for gas sensor application. Thus there are abundance of possibilities to combine these 2D nanomaterials to construct 2D/2D nanocomposites as new po-

tential sensor material. Second, the synergetic effect arise from 2D/2D composition could be further enhanced by elaborate design. For example, the formation of II type heterostructure using semiconducting 2D nanomaterials could facilitate the charge separation that improve the gas molecule adsorption and accelerate the reaction. Hybridizing photosensitive TMDCs with gas sensitive materials could improve the adsorption and desorption of gas molecules upon light irradiation owing to the illumination induced high-concentration charge carriers. Third, reported literatures have demonstrated that the sensing properties of well-designed ternary 2D nanocomposites surpass that of binary 2D nanocomposites. This is because adding new component could provide a new dimension for sensing modulation. Thus, developing multielement 2D nanocomposites would be an efficient approach to exploit next-generation high-performance, flexible, and low power consumption sensor devices.

Acknowledgments

This work was supported by Zhejiang Provincial Natural Science Foundation of China (No. LY18F010009) and Ningbo Natural Science Foundation (No. 2018A610002).

References

[1] Yamazoe N. Toward innovations of gas sensor technology. Sens Actuators B, 2005, 108(1/2), 2
[2] Kohl D. Function and applications of gas sensors. J Phys D, 2001, 34(19), 125
[3] Lee E, Yoon Y S, Kim D J. Two-dimensional transition metal dichalcogenides and metal oxide hybrids for gas sensing. ACS Sens, 2018, 3(10), 2045
[4] Wang C, Cui X, Liu J, et al. Design of superior ethanol gas sensor based on Al-doped NiO nanorod-flowers. ACS Sens, 2015, 1(2), 131
[5] Zhang Q, Wang X, Fu J, et al. Electrospinning of ultrafine conducting polymer composite nanofibers with diameter less than 70 nm as high sensitive gas sensor. Materials (Basel), 2018, 11(9), 1744
[6] Ngo Y H, Brothers M, Martin J A, et al. Chemically enhanced polymer-coated carbon nanotube electronic gas sensor for isopropyl alcohol detection. ACS Omega, 2018, 3(6), 6230
[7] Suematsu K, Shin Y, Ma N, et al. Pulse-driven micro gas sensor fitted with clustered Pd/SnO_2 nanoparticles. Anal Chem, 2015, 87(16), 8407
[8] Zhang S, Nguyen S, Nguyen T, et al. Effect of the morphology of solution-grown ZnO nanostructures on gas-sensing properties. J Am Ceram Soc, 2017, 100, 5629
[9] Ghoorchian A, Alizadeh N. Chemiresistor gas sensor based on sulfonated dye-doped modified conducting polypyrrole film for high sensitive detection of 2, 4, 6-trinitrotoluene in air. Sens Actuators B, 2018, 255, 826
[10] Ong K, Zeng K, Grimes C. A wireless, passive carbon nanotube-based gas sensor. IEEE Sens J, 2002, 2(2), 82
[11] Ponomarenko L, Gorbachev R, Yu G, et al. Cloning of Dirac fermions in graphene superlattices. Nature, 2013, 497(7451), 594
[12] Schedin F, Geim A, Morozov S, et al. Detection of individual gas molecules adsorbed on graphene. Nat Mater, 2007, 6(9), 652
[13] Liu X, Ma T, Pinna N, et al. Two-dimensional nanostructured materials for gas sensing. Adv Funct Mater, 2017, 27(37), 1702168
[14] Zhang S, Nguyen T H, Zhang W, et al. Correlation between lateral size and gas sensing performance of $MoSe_2$ nanosheets. Appl Phys Lett, 2017, 111, 161603
[15] Song Z, Fan Y, Sun Z, et al. A new strategy for integrating superior mechanical performance and high volumetric energy density into a Janus graphene film for wearable solid-state supercapacitors. J Mater Chem A, 2017, 5(39), 20797
[16] Zhang S, Zhang Z, Yang W. High-yield exfoliation of graphene using ternary-solvent strategy for detecting volatile organic compounds. Appl Surf Sci, 2016, 360, 323
[17] Tan L, Li N, Chen S, et al. Self-assembly synthesis of CuSe@graphene–carbon nanotubes as efficient and robust oxygen reduction electrocatalysts for microbial fuel cells. J Mater Chem A, 2016, 4(31), 12273
[18] Chen G, Kou X, Huang S, et al. Allochroic-graphene oxide linked 3D oriented surface imprinting strategy for glycoproteins assays. Adv Funct Mater, 2018, 28(40), 1804129
[19] Varghese S, Varghese S, Swaminathan S, et al. Two-dimensional materials for sensing: graphene and beyond. Electronics, 2015, 4(3), 651
[20] Choi W, Choudhary N, Han G H, et al. Recent development of two-dimensional transition metal dichalcogenides and their applications. Mater Today, 2017, 20(3), 116
[21] Zhao R, Wang T, Zhao M, et al. External electric field and strains facilitated nitrogen dioxide gas sensing properties on 2D monolayer and bilayer SnS_2 nanosheets. Appl Surf Sci, 2019, 491, 15
[22] Järvinen T, Lorite G S, Peräntie J, et al. WS_2 and MoS_2 thin film gas sensors with high response to NH_3 in air at low temperature. Nanotechnology, 2019, 30(40), 405501
[23] Singh E, Meyyappan M, Nalwa H S, et al. Flexible graphene-based wearable gas and chemical sensors. ACS Appl Mater Inter, 2017, 9(40), 34544
[24] Mackin C, Schroeder V, Zurutuza A, et al. Chemiresistive graphene sensors forammonia detection. ACS Appl Mater Inter, 2018, 10(18), 16169
[25] Donarelli M, Ottaviano L J. 2D materials for gas sensing applications: A review on graphene oxide, MoS_2, WS_2 and phosphorene. Sensors, 2018, 18(11), 3638
[26] Zhang S, Zhang W, Nguyen T, et al. Synthesis of molybdenum diselenide nanosheets and its ethanol-sensing mechanism. Mater Chem Phys, 2019, 222, 139
[27] Kim T H, Kim Y H, Park S Y, et al. Two-dimensional transition metal disulfides for chemoresistive gas sensing: perspective and challenges. Chemosensors, 2017, 5(2), 15
[28] Joshi N, Hayasaka T, Liu Y, et al. A review on chemiresistive room temperature gas sensors based on metal oxide nanostructures, graphene and 2D transition metal dichalcogenides. Microchim Acta, 2018, 185(4), 213
[29] Jariwala D, Sangwan V K, Lauhon L J, et al. Emerging device applications for semiconducting two-dimensional transition metal dichalcogenides. ACS Nano, 2014, 8(2), 1102
[30] Jang J S, Lee S E, Choi S J, et al. Heterogeneous, porous 2D oxide sheets via rapid galvanic replacement: toward superior HCHO sensing application. Adv Funct Mater, 2019, 29(42), 1903012
[31] Zhang S, Hang N, Zhang Z, et al. Preparation of g-C_3N_4/graphene composite for detecting NO_2 at room temperature. Nanomaterials, 2017, 7(1), 12
[32] Hang N T, Zhang S, Yang W J, et al. Efficient exfoliation of g-C_3N_4 and NO_2 sensing behavior of graphene/g-C_3N_4 nanocomposite. Sens Actuators B, 2017, 248, 940
[33] Choi S J, Kim I D. Recent developments in 2D nanomaterials for chemiresistive-type gas sensors. Electron Mater Lett, 2018, 14(3), 221
[34] Yang W, Gan L, Li H, et al. Two-dimensional layered nanomaterials for gas-sensing applications. Inorg Chem Front, 2016, 3(4), 433
[35] Yu X, Cheng H, Zhang M, et al. Graphene-based smart materials. Nat Rev Mater, 2017, 2(9), 17046
[36] Lu G, Park S, Yu K, et al. Toward practical gas sensing with highly reduced graphene oxide: a new signal processing method to cir-

cumvent run-to-run and device-to-device variations. ACS Nano, 2011, 5(2), 1154

[37] Yuan W, Shi G J. Graphene-based gas sensors. J Mater Chem, 2013, 1(35), 10078

[38] Hubble L J, Cooper J S, Pintos A S, et al. High-throughput fabrication and screening improves gold nanoparticle chemiresistor sensor performance. ACS Comb Sci, 2015, 17(2), 120

[39] Davis C, Ho C, Hughes R, et al. Enhanced detection of m-xylene using a preconcentrator with a chemiresistor sensor. ACS Comb Sci, 2005, 104(2), 207

[40] Mohanty N, Berry V. Graphene-based single-bacterium resolution biodevice and DNA transistor: interfacing graphene derivatives with nanoscale and microscale biocomponents. Nano Lett, 2008, 8(12), 4469

[41] Cho S Y, Kim S J, Lee Y, et al. Highly enhanced gas adsorption properties in vertically aligned MoS_2 layers. ACS Nano, 2015, 9(9), 9314

[42] Ma J, Zhang M, Dong L, et al. Gas sensor based on defective graphene/pristine graphene hybrid towards high sensitivity detection of NO_2. AIP Advan, 2019, 9(7), 075207

[43] Yu W J, Li Z, Zhou H, et al. Vertically stacked multi-heterostructures of layered materials for logic transistors and complementary inverters. Nat Mater, 2013, 12(3), 246

[44] Choi M S, Lee G H, Yu Y J, et al. Controlled charge trapping by molybdenum disulphide and graphene in ultrathin heterostructured memory devices. Nat Commun, 2013, 4, 1624

[45] Cho B, Yoon J, Lim S K, et al. Chemical sensing of 2D graphene/MoS_2 heterostructure device. ACS Appl Mater Inter, 2015, 7(30), 16775

[46] Zhang S L, Yue H, Liang X, et al. Liquid-phase Co-exfoliated graphene/MoS_2 nanocomposite for methanol gas sensing. J Nanosci Nanotechnol, 2015, 15(10), 8004

[47] Long H, Trochimczyk A, Pham T, et al. High surface area MoS_2/graphene hybrid aerogel for ultrasensitive NO_2 detection. Adv Funct Mater, 2016, 26(28), 5158

[48] Tabata H, Sato Y, Oi K, et al. Bias-and gate-tunable gas sensor response originating from modulation in the Schottky barrier height of a graphene/MoS_2 van der Waals heterojunction. ACS Appl Mater Inter, 2018, 10(44), 38387

[49] Zhou Y, Lin X, Huang Y, et al. Impact of further thermal reduction on few-layer reduced graphene oxide film and its np transition for gas sensing. Sens Actuators B, 2016, 235, 241

[50] Sun Q, Wu Z, Duan H, et al. Detection of triacetone triperoxide (TATP) precursors with an array of sensors based on MoS_2/RGO composites. Sensors, 2019, 19(6), 1281

[51] Kumar R, Dias W, Rubira R J, et al. Simple and fast approach for synthesis of reduced graphene oxide–MoS_2 hybrids for room temperature gas detection. IEEE Trans Electron Devices, 2018, 65(9), 3943

[52] Jung M W, Kang S M, Nam K H, et al. Highly transparent and flexible NO_2 gas sensor film based on MoS_2/rGO composites using soft lithographic patterning. Appl Surf Sci, 2018, 456, 7

[53] Zhou Y, Liu G, Zhu X, et al. Ultrasensitive NO_2 gas sensing based on rGO/MoS_2 nanocomposite film at low temperature. Sens Actuators B, 2017, 251, 280

[54] Li X, Wang J, Xie D, et al. Reduced graphene oxide/MoS_2 hybrid films for room-temperature formaldehyde detection. Mater Lett, 2017, 189, 42

[55] Sun J, Lin N, Ren H, et al. Gas adsorption on MoS_2/WS_2 in-plane heterojunctions and the *I*–*V* response: A first principles study. RSC Adv, 2016, 6(21), 17494

[56] Paolucci V, Emamjomeh S M, Ottaviano L, et al. Near room temperature light-activated WS_2-decorated rGO as NO_2 gas sensor. Sensors, 2019, 19(11), 2617

[57] Li X, Wang J, Xie D, et al. Flexible room-temperature formaldehyde sensors based on rGO film and /MoS_2 hybrid film. Nanotechnology, 2017, 28(32), 325501

[58] Yoon H J, Yang J H, Zhou Z, et al. Carbon dioxide gas sensor using a graphene sheet. Sens Actuators B, 2011, 157(1), 310

[59] Shih C, Wang Q, Son Y, et al. Tuning on–off current ratio and field-effect mobility in a MoS_2–graphene heterostructure via Schottky barrier modulation. ACS Nano, 2014, 8(6), 5790

[60] Han C, Chen Z, Zhang N, et al. Hierarchically CdS decorated 1D ZnO nanorods-2D graphene hybrids: low temperature synthesis and enhanced photocatalytic performance. Adv Funct Mater, 2015, 25(2), 221

[61] Ikram M, Liu L, Liu Y, et al. Fabrication and characterization of a high-surface area MoS_2@WS_2 heterojunction for the ultra-sensitive NO_2 detection at room temperature. J Mater Chem A, 2019, 7(24), 14602

[62] Shao S, Che L, Chen Y, et al. A novel RGO-MoS_2-CdS nanocomposite film for application in the ultrasensitive NO_2 detection. J Alloy Compd, 2019, 774, 1

[63] Shi S, Hu R, Wu E, et al. Highly-sensitive gas sensor based on two-dimensional material field effect transistor. Nanotechnology, 2018, 29(43), 435502